Analysis of the NO_x formation pathways in a partially premixed burner operated with pure hydrogen

R. Meloni*, G. Babazzi*, L. Mazzotta*,, D. Borello*****
roberto.meloni@bakerhughes.com
*Baker Hughes, Via F. Matteucci 2, 50127, Florence, Italy
**Department of Astronautical, Electric and Energetic Engineering, Sapienza University of Rome, Via Eudossiana 18, Rome, 00184, Italy
***Department of Mechanical and Aerospace Engineering, Sapienza University of Rome, Via Eudossiana 18, Rome, 00184, Italy

Abstract
The need of reliable CFD models able to predict the performance of pure hydrogen combustion is becoming strategic for the development of new burner designs for GT. So, in this research paper, the results of a species-transport based model applied to the HYLON burner will be presented. Both the attached and the lifted flame configuration are investigated and discussed showing an excellent agreement with the experimental measurements. Furthermore, the CFD solutions are coupled with a CRN to estimate the NO_x emission, considering all the possible formation pathways.

Introduction
Hydrogen combustion represents one of the biggest challenge gas turbine manufacturers have to deal with, especially in the context of low NO_x emissions. The hitch consists in finding a design able to guarantee low emissions avoiding thermo-acoustic instabilities as well as flashback/flame holding [1]. An additional roadblock in the design space is represented by the lack of reliability of the CFD models for hydrogen combustion. Computationally cheap models based on pre-tabulated chemistry are totally unreliable since they are not able to capture some fundamental hydrogen properties (i.e., response to the strain rate, preferential diffusion). On the other side, models relying on the species transport, despite their high computational costs, are not free of uncertainties when applied to high-pressure and high-temperature conditions. It must be also considered that detailed measures able to characterize a pure hydrogen flame at these conditions are totally missing in literature. This deficiency is limiting the assessment of the actual prediction capabilities of the numerical models for industrial applications. More often instead, their validation must leverage single-swirler tests at low pressure where the optical access allows the execution of quantitative measures. Radical chemiluminescence and PIV can be performed to fully characterize the flame length and its morphology providing crucial information for the optimization of the numerical models. The same kind of approach is presented in this work for the HYLON burner [2]. The prediction capabilities of a species transport-based model will be evaluated comparing the numerical results against detailed measures. An insight on the NO_x

emission for the two investigated operating conditions will be discussed as well.

Test Rig and Computational Mesh Resolution

The computational domain is prepared referring to the material reported in [2] where also the operating conditions characterizing the burner in the *Attached* (*A*) and *Lifted* (*L*) configuration are detailed. Figure 1-a shows the employed geometry with a close up of the HYLON burner, unveiling the details of both the radial passages of the air and the fuel line. The latter is characterized by a swirler mounted close to the burner exit providing an additional swirler that enhances the flame stabilization in the primary zone. Instead, Figure 1-b reports the size of the computational mesh in the most important regions of the model. The finest mesh resolution, equal to about 50 µm, is applied in the final part of the burner and where the flame gets stabilized in the primary zone as demonstrated by the contour plot of the normalized HRR for the flame *A*. The mesh remains extremely fine (~300 µm) right outside these regions and progressively coarser elsewhere, reaching a maximum of 600 µm. The total mesh count is of approximately 25 million polyhedral elements.

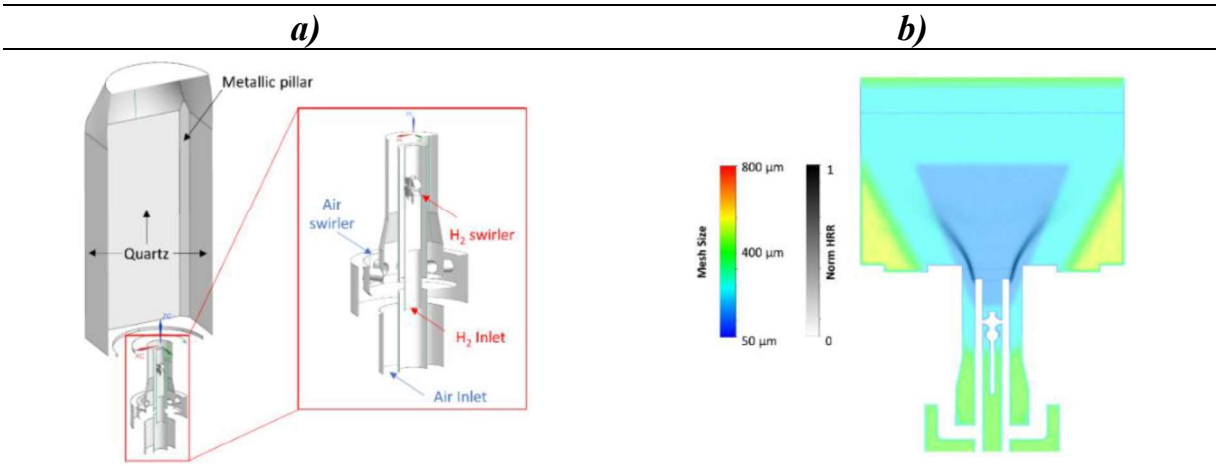

Figure 1. *Combustion test rig with detailed view of the HYLON burner (a) and mesh inside the swirler and the primary zone (b).*

As it will be discussed in the next paragraph, the grid plays a crucial role in the performance of the combustion model in the large-eddy simulation context. This mesh is able not only to resolve most of the turbulent length scales, as demonstrated by Aniello et al. [3] where a similar discretization strategy is adopted, but it can also accurately model the diffusive and the premixed regime both present in a stratified flame. While the former requires a high resolution to properly capture the mixing among species, the premixed regime needs a fine mesh to accurately reconstruct the species profiles in the flame front thickness, according to the TFM [4].

Enhanced-Thickened Flame Model and Numerical Settings

The closure of the chemical source term of each species transport equation depends on the local value of the flame index, calculated according to Eq. 1:

$$FI = \frac{\nabla Y_{H2} \cdot \nabla Y_{O2}}{|\nabla Y_{H2} \cdot \nabla Y_{O2}|} \quad (1)$$

If the FI is negative (diffusive regime), the finite rate closure is adopted, while the TFM formulation is applied for positive values (premixed flame), characterized by a fixed flame propagation speed and a chemically controlled fuel consumption. So, the formulation of the transport equation of each species $\tilde{\varphi}$ can be written as:

$$\frac{\partial \bar{\rho}\,\tilde{\varphi}}{\partial t}+\frac{\partial \bar{\rho}\,\widetilde{u_j}\,\tilde{\varphi}}{\partial x_j} = \frac{\partial}{\partial x_j}\left(\bar{\rho}(EFD + (1-\Omega)D_t)\frac{\partial \tilde{\varphi}}{\partial x_j}\right)+\frac{E}{F}\dot{\omega}(\tilde{\varphi}) \quad (2)$$

with E and F the efficiency function and the thickening factor, respectively. These two parameters are simply set to unity for $FI < 0$ or calculated by a user-defined function according to the Colin's formulation for E [4] and Eq. 3 for F:

$$F = \Omega(F_{max} - 1) + 1 \quad (3)$$

The maximum thickening factor is calculated as $F_{max} = \Delta x\, N/LFT(\Phi)$. The actual mesh resolution (Fig. 1-b), Δx, can limit F_{max} to values close to 5 having chosen a number of points $N = 10$ inside the flame front thickness ($LFT(\Phi)$). The flame front is identified through the sensor Ω, calculated considering $H_2 + OH \rightarrow H_2O + H$ as reference reaction. The reduced mechanism by Boivin et al. [5] made of 9 species and 12 reactions is used. Mass flow rates are imposed at air and H_2 inlets while a pressure outlet is placed at the end of the quartz. The temperature at the metallic pillars and at quartz liner are adopted according to the measured data.

Results and Discussion

Flame morphology

The comparison between the experiments and numerical model in terms of flame shape and position is reported in Figure 2, showing the HRR for the former and the OH* for the latter. The CFD is able to predict both the flame configurations varying the overall air mass flow rate. Flame A is characterized by the anchoring of the flame root at the lip of the hydrogen injector where, as demonstrated by Aniello et al. [4], the fuel is trapped by a local recirculation eventually leading the heat release region to be confined between the shear layer and the external recirculation zone. The combustion model can also correctly predict the weak HRR in the core of the swirler flow, downstream the H_2 injector, barely visible in Figure 2-a. Conversely, the higher air bulk velocity in Flame L overcomes the local laminar flame speed at the H_2 lip preventing the flame stabilization and promoting a lift-off. Also, the location of the OH* peak is well captured.

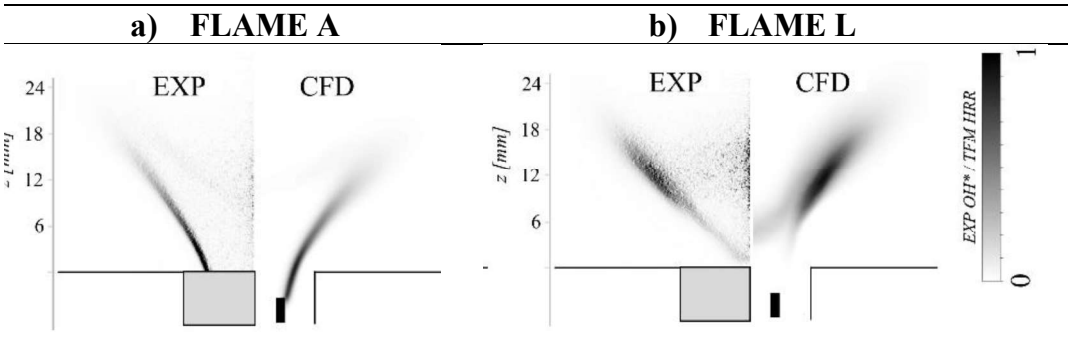

Figure 2. *Experimental Abel-deconvoluted OH* vs CFD HRR for flame A (a) and L (b).*

Figure 3 shows the HRR conditioned with the flame index at the stoichiometric iso-surface: while Flame A burns totally in diffusive mode anchored to the H_2 injector, Flame L has a mixed combustion regime: the flame lift-off gives H_2 sufficient time to mix with a benefit in terms of NO_x reduction [3].

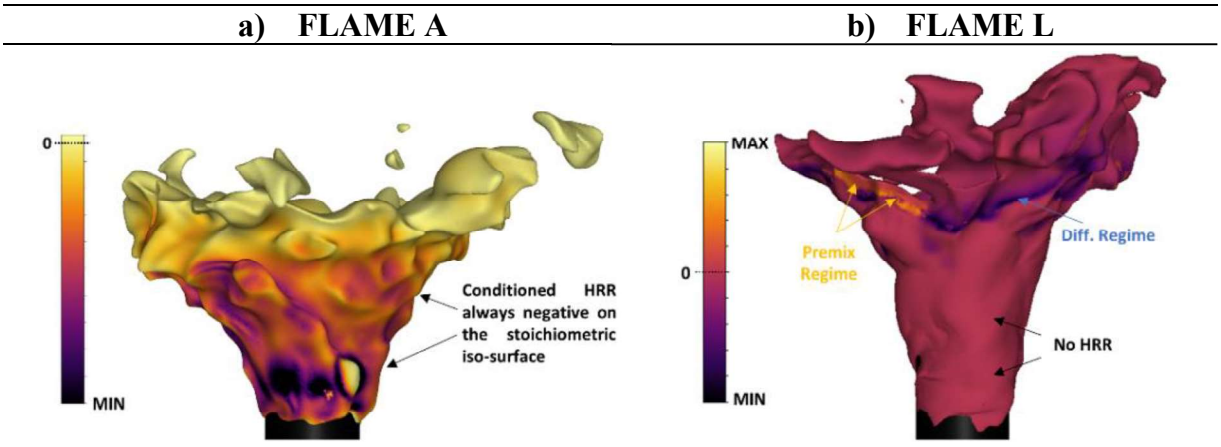

Figure 3. *Instantaneous normalized FI- conditioned HRR for Flame A (a) and L (b).*

Reactive velocity profiles

For sake of brevity, only the contour plots of velocity magnitude and axial velocity profiles at $z = 5$ and $z = 15\,mm$, reported in Figure 4, are here discussed. Regarding the velocity magnitude fields, the opening angle of the swirled air as well as the interaction of the jets with the walls are quite well predicted in both conditions. Some minor differences are present for Flame L. First of all, a more intense central recirculation zones is obtained: this can be observed also from the radial velocity profiles at low x-coordinate values. Additionally, the numerical results show also a more axially extended high velocity field closer to the walls. These small differences for the lifted flame could be related to the outlet boundary placed at the end of the quartz without considering any interaction with the atmosphere outside the flame tube that can play a role when the mass flow rate is increased. On the other side, the radial profiles for Flame A seems not have relevant discrepancies against the PIV. While there is an overlapping of the numerical with the experimental results at $z = 5$ mm, a small underprediction of the peak velocity is found at $z = 15$ mm.

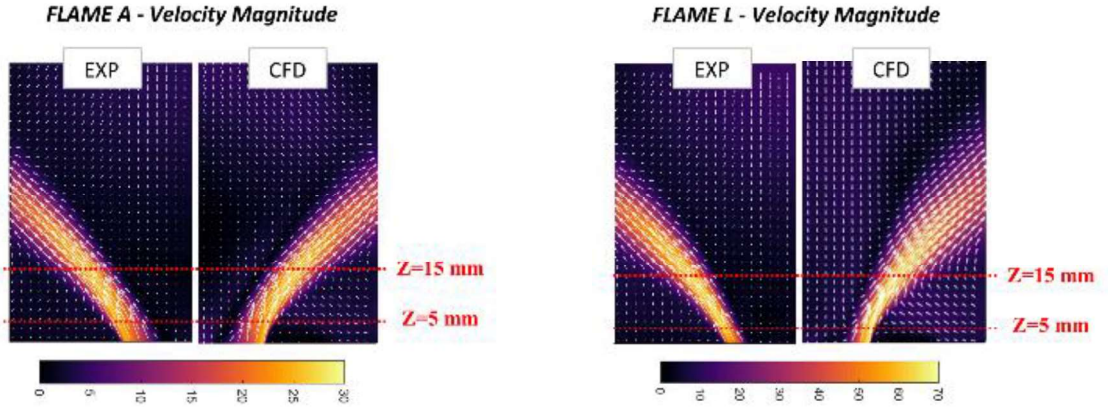

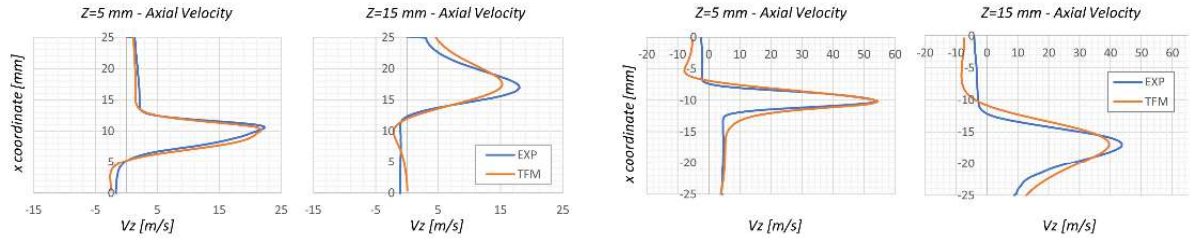

Figure 4. *Velocity profiles comparison in reactive conditions.*

CFD-CRN methodology and results

The CFD-CRN methodology is used to quantify NO_x emissions in the exhaust section. It is a simplified approach for analysing complex systems, such as those typical of gas turbines and perform a wide range of sensitivity to several parameters. Figure 5 shows the different reactors through which both flames are schematized.

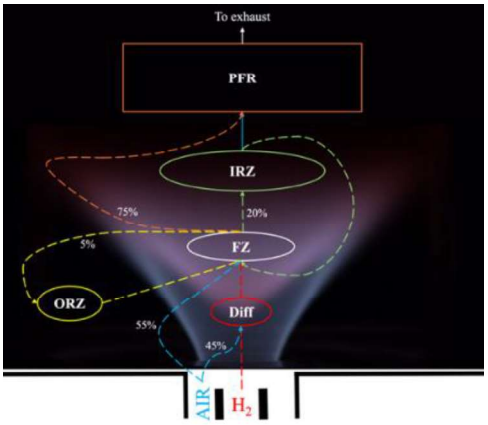

Figure 5. *CRN scheme adopted to quantify NO_x for both flames.*

Three PSRs representing the FZ and the two recirculation zones (IRZ and ORZ) are employed. A diffusion zone is used to consider the formation of the high temperature in the flame front. This zone is obtained by splitting the air to obtain the stoichiometric equivalence ratio. Additionally, a PFR denotes the inclusion of a unidirectional flow zone. By analysing the axial velocity field and HRR from the LES, it is possible to obtain the volumes to be associated to the FZ and I/ORZs, respectively and obtain the residence times of each zone. The split percentages between the different volumes are obtained by CFD. The kinetic scheme of Stagni et al. [6] was used, with all the main reactions characterizing NO_x formation within it. Figure 6b demonstrates that the NO emission derived from the LES-CRN analysis are predicted with an error of less than 4%. To assess the consumption and production contributions of the main reactions derived from the NO_x formation mechanisms (thermal and NNH) of both flames (A and L), the ROP values were compared within the flame zone, as shown in Figures 6a,c. High flame temperature (greater than 1850 K) promotes the NO formation in the burnt gases through the Zeldovich route and the residence time will determine the NO concentrations. In fact, $N+NO <=> O+N_2$ results the main reaction responsible for the NO reduction, as shown in Fig. 6c, while consumption of NNH prevails for the lifted flame.

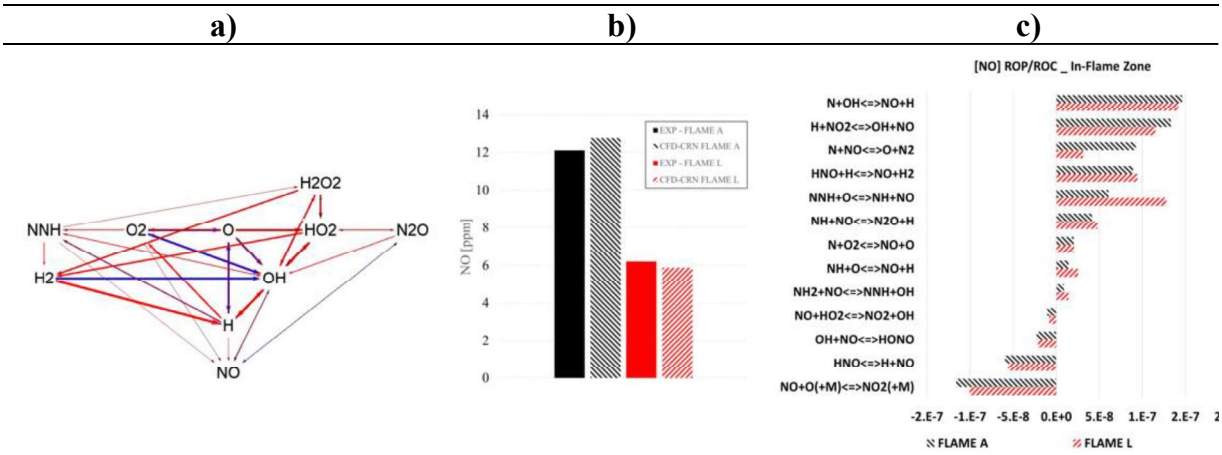

Figure 6. *(a) NO formation pathway in the FZ; (b) NO emissions results: LES-CRN vs data; (c) absolute ROP [mole/cm^3-sec] for the main NO reactions inside the FZ.*

Conclusion

In the present work, the results of a customized TFM are compared with detailed measures of the HYLON burner. The findings characterizing the flame front are in line with the experimental OH* maps for both the attached and lifted flame configuration. Also the reactive flow fields are in good agreement with the PIV data. A CRN for the assessment of the NO emission is built on top of the CFD solution, providing a good agreement with the experimental measures for both flames.

Nomenclature

CFD	*Computational Fluid Dynamics*	*HRR*	*Heat Release Rate*
CRN	*Chemical Reactor Network*	*PIV*	*Particle Image Velocimetry*
FI	*Flame Index*	*TFM*	*Thickened Flame Model*
PFR	*Plug Flow Reactor*	*PSR*	*Perfectly Stirred Reactor*
ORZ	*Outer Recirculation Zone*	*IRZ*	*Inner Recirculation Zone*
ROP	*Rate Of Production*	*FZ*	*Flame Zone*

References

[1] T. Lieuwen, Y. Neumeier, B. T. Zinn (1998). *"The Role of Unmixedness and Chemical Kinetics in Driving Combustion Instabilities in Lean Premixed Combustors"*, Comb. Science and Technology, 135:1-6, 193-211

[2] https://tnfworkshop.org/hydrogen-flames/

[3] A. Aniello, D. Laera, S. Marragou, H. Magnes, L. Selle, T. Schuller, T. Poinsot, *"Experimental and numerical investigation of two flame stabilization regimes observed in a dual swirl H2-air coaxial injector"*, Comb. Flame, Vol. 249, 2023

[4] O. Colin, F. Ducros, D. Veynante, T. Poinsot, *"A thickened flame model for large eddy simulations of turbulent premixed combustion"*, *Phys. Fluids 12* (2000) 1843-63

[5] P. Boivin, C. Jiménez, A.L. Sánchez, F.A. Williams, "An explicit reduced mechanism for H_2–air combustion", Proceedings of the Combustion Institute, Vol 33, 2011.

[6] Stagni, A., Cavallotti, C., Arunthanayothin, S., Song, Y., Herbinet, O., Battin-Leclerc, F., and Faravelli, T., 2020. "*An experimental, theoretical and kinetic-modelling study of the gas-phase oxidation of ammonia*". React. Chem. Eng., 5, pp. 696–711